JOURNAL OF Materials CHEMISTRY

Symmetric and asymmetric charge transfer process of two-photon absorbing chromophores: bis-donor substituted stilbenes, and substituted styrylquinolinium and styrylpyridinium derivatives

XiaoMei Wang, Dong Wang, GuangYong Zhou, WenTao Yu, YuFang Zhou, Qi Fang and MinHua Jiang*

State Key Laboratory of Crystal Materials, Shandong University, Jinan 250100, P. R. China. E-mail: mhjiang@sdu.edu.cn; Fax: (+86)-0531-8564550; Tel: (+86)-0531-8564550

Received 6th December 2000, Accepted 27th March 2001
First published as an Advance Article on the web 30th April 2001

Two-photon absorption properties of a series of symmetrically substituted stilbenes and asymmetrically substituted stilbene-type derivatives with the same conjugated length have been investigated. The effective two-photon absorption cross sections, δ_{TPA}, as large as 62.0×10^{-48} cm^4 s photon^{-1} for D-π-D molecules and 48.5×10^{-48} cm^4 s photon^{-1} for D-π-A counterparts have been observed. The effect of these two types of chromophores on the peak position of the linear absorption, one-photon fluorescence as well as two-photon absorptivity is reported. Dipole moment change between the ground and the first excited states ($\Delta\mu_{ge}$), and the transition dipole moment between the first and second excited states ($M_{ee'}$) have also been calculated. It was found that the asymmetrically substituted derivatives possess relatively large $\Delta\mu_{ge}$, whereas the symmetrical counterparts show an increase in $M_{ee'}$. Although a large two-photon absorption resonance is due to the simultaneously high values of $M_{ee'}$ and $\Delta\mu_{ge}$, correlated to intramolecular charge transfer, the former function is larger. These results obtained have demonstrated that the magnitude and the peak position of two-photon absorption depend not only on the amount but also on the direction of the intramolecular charge transfer.

Introduction

Two-photon absorption (TPA) is a nonlinear optical process, which can be described theoretically by either the two-state model[1] or the three-state model,[2,3] that a molecule can be excited from the ground state (S_0) to the first excited singlet state (S_1) or to the second excited singlet state (S_2) by simultaneous absorption of two photons, (*i.e.* $\Delta E_{S0\text{-}S1} = 2h\nu_1$, or $\Delta E_{S0\text{-}S2} = 2h\nu_2$). At present, the exploration of new applications requires a better understanding of the relationship between molecular structure and two-photon absorption (TPA) properties. It is reported that many organic molecules exhibit strong optical power limiting behavior resulting from two-photon absorption (TPA).[4–6] Two-photon polymerization initiators for three-dimensional optical data storage could improve the spatial resolution in the microfabrication.[7,8] Three-dimensional fluorescence imaging,[9] lithographic microfabrication,[10,11] laser device fabrication,[12–14] two-photon photodynamic therapy[1,15] and two-photon pumped up-conversion lasing[16–18] are other promising applications for the TPA property of organic molecules. This potential of using two-photon absorbing molecules in applications has inevitably stimulated research on the design, synthesis, and characterization of new molecules with large two-photon absorptivities. The ultimate goal is to determine the relationship between molecular structure and the TPA property so as to optimize the choice of application oriented molecules. In the exploration of strong TPA compounds, Albota *et al.*[2] have focused on symmetric organic compounds and reported a design strategy for symmetrically substituted conjugated molecules (D-π-D type), while Reinhardt *et al.*[19] have emphasized the D-π-A type chromophores. The former emphasized the importance of conjugation length and molecular symmetry, while the latter laid stress on the planarity of π-center and donor–acceptor strength. Therefore, there is an increasing need to understand in detail about the influence of molecular symmetry on molecular two-photon absorption properties, to guide the design of molecules whereby one can systematically increase the TPA cross section and tune the position of the two-photon absorption peak. The development of such a structure–property relationship not only is greatly beneficial to the design of new materials, but also makes these materials suitable for the applications given.

We have reported previously on a series of D-π-A asymmetric chromophores, and investigated their two-photon absorptivities[20] and two-photon-pumped emission[21] under the 1064 nm mode-locked Nd:YAG laser pulse. Experimental and theoretical evidence have shown that the amount of intramolecular charge transfer makes a positive contribution to enhancing both the TPA cross section and the up-conversion lasing efficiency. In this paper, a comparative study of the two-photon absorption property for symmetrically and asymmetrically substituted chromophores is reported for understanding the relationship between the symmetric and asymmetric charge transfer process and molecular two-photon absorption. The results we report in this paper are as follows: (1) One-photon absorption and fluorescence emission as well as the solvent effects for symmetrically and asymmetrically substituted chromophores are discussed. (2) An examination of how the transition dipole moment ($M_{ee'}$) and dipole moment change ($\Delta\mu_{ge}$) as well as the charge density distribution vary with the molecular symmetry is presented. (3) The effect of symmetric molecules on the peak position and magnitude of the two-photon absorption has been studied by comparison. The molecular structures considered are shown in Fig. 1.

Experimental section

Materials

The molecules shown in Fig. 1 possess "D-B-D" and "D-B-A" structures with the same conjugated length, where "D" is a tertiary amino electron-donating group, "A" is an *N*-methylpyridinium iodide or a *N*-methylquinolinium iodide, "B" is a stilbene bridge for symmetric molecules and a styryl

 DOI: 10.1039/b009769l

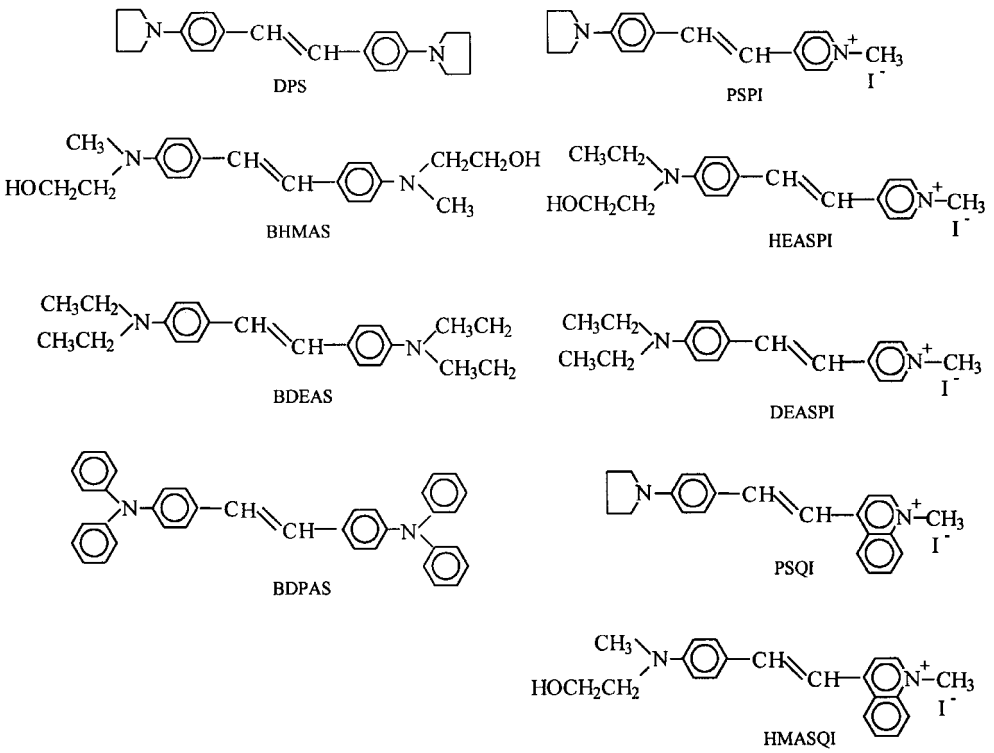

Fig. 1 Molecular structures of the D-π-D and D-π-A chromophores discussed in this paper.

bridge for asymmetric molecules, respectively. Here, the new "D-π-D" chromophores were firstly synthesized by Ti-catalyzed reductive coupling of *p*-substituted aminobenzaldehydes and have been characterized by X-ray diffraction, mass spectra and elemental analyses with the same methods as reported previously.[20] The syntheses of "D-π-A" molecules in Fig. 1 have been reported.[20]

Synthesis of symmetrically substituted stilbene derivatives. Under anhydrous and oxygen-free conditions, a mixture of $TiCl_4$ (2.2 mL, 20 mmol), zinc (4.4 g, 60 mmol), sodium metal (2.3 g, 100 mmol) and 75 mL of dry tetrahydrofuran (THF) was stirred in a flask at room temperature. After refluxing for one hour, a black mixture was obtained, which was then cooled to room temperature. A solution of 4-pyrrolidin-1-ylbenzaldehyde[21] was added slowly to the flask and further refluxed for 20 h. The mixture was then cooled, hydrolyzed by adding dropwise 5% HCl and neutralized by using 2 M sodium hydroxide solution, respectively. The mixture was extracted with chloroform. The organic layer was concentrated by evaporation and purified by column chromatography on silica gel using appropriate solvent as eluent. After evaporation, (*E*)-4,4′-di(pyrrolidinyl)stilbene, (**DPS**) green–yellow crystals were obtained with a yield of 65% and mp 298.9 °C. Mass spectrum, *m*/*z* 318 (M^+), 289, 275, 262, 159. Elemental analysis: Calcd.: C, 82.97; H, 8.23; N, 8.80. Found: C, 83.36; H, 7.88; N, 8.45%.

Replacing 4-pyrrolidin-1-ylbenzaldehyde with 4-(*N*,*N*-diphenylamino)benzaldehyde, 4-(*N*,*N*-diethylamino)benzaldehyde, and 4-[(*N*-hydroxyethyl-*N*-methyl)amino]benzaldehyde, respectively, the following chromophores were obtained.

(*E*)-4,4′-Bis(diphenylamino)stilbene (**BDPAS**): Bright yellow slice crystals. Yield 60% and mp 255.9 °C. Mass spectrum, *m*/*z* 514 (M^+), 257, 167, 77. Elemental analysis: Calcd.: C, 88.68; H, 5.88; N, 5.44. Found: C, 88.94; H, 5.58; N, 5.36%.

(*E*)-4,4′-Bis(diethylamino)stilbene (**BDEAS**): Yellow slice crystals with yield 54%. Mass spectrum, *m*/*z* 322 (M^+), 307, 278, 263, 146. Elemental analysis: Calcd.: C, 81.94; H, 9.38; N, 8.69. Found: C, 81.45; H, 9.58; N, 8.36%.

(*E*)-4,4′-Bis(*N*-hydroxyethyl-*N*-methylamino)stilbene (**BHMAS**): Green–yellow needle crystals with yield of 50% and mp 172.0 °C. Mass spectrum, *m*/*z* 326 (M^+), 295, 249, 132. Elemental analysis: Calcd.: C, 73.59; H, 8.03; N, 8.58. Found: C, 73.15; H, 8.42; N, 8.91%.

Crystal structure. The molecular structures of BDPAS and DPS and their packing diagram are shown in Figs. 2–5, respectively. The BDPAS crystal belongs to the triclinic crystal system of centrosymmetric space group $P\bar{1}$ with unit cell parameters of $a=10.6231(12)$, $b=11.3337$ (10), $c=12.491(3)$ Å, $\alpha=73.503$ (9), $\beta=89.978$ (10), $\gamma=79.759$ (8)°. Least-square plane calculations show that the central stilbene unit possesses perfect planarity, but two terminal benzene rings deviate from both central stilbene planarity and themselves. For example, the dihedral angles between each terminal benzene ring and the central stilbene unit are 102.2 and 106.4°, respectively, while that between two terminal benzene rings is 61.8°. The packing diagram shows that the BDPAS molecules stack in pairs, aligning at 45° to the *b* axis and *c* axis.

The DPS crystal belongs to a monoclinic crystal system of centrosymmetric space group $P2_1/c$ with unit cell parameters of $a=6.5813(6)$, $b=7.7337(7)$, $c=17.6791(16)$ Å, $\alpha=90$, $\beta=105.268(7)$, $\gamma=90°$. The packing diagram shows that the DPS

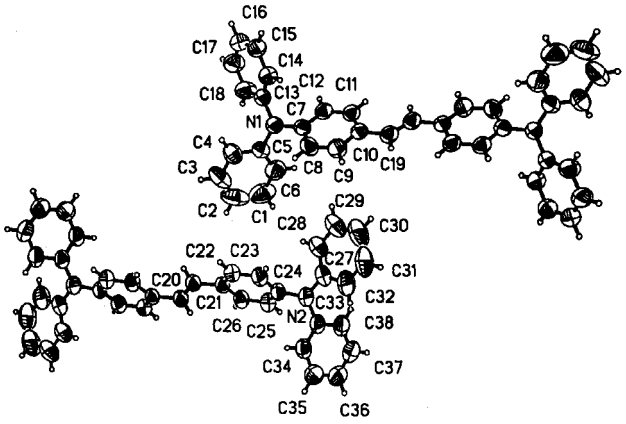

Fig. 2 The molecular structure of BDPAS crystal.

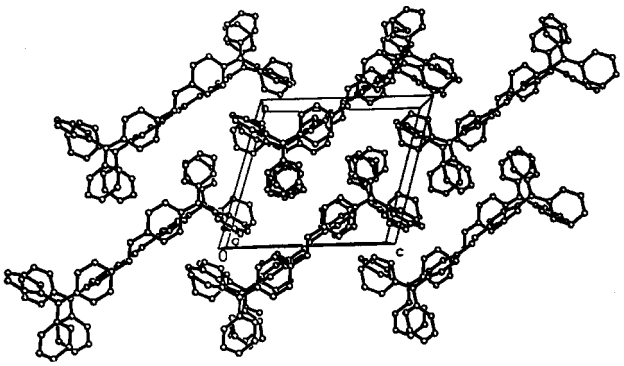

Fig. 3 Packing diagram of BDPAS.

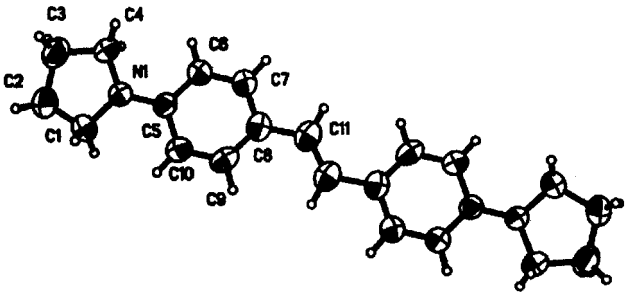

Fig. 4 The molecular structure of DPS crystal.

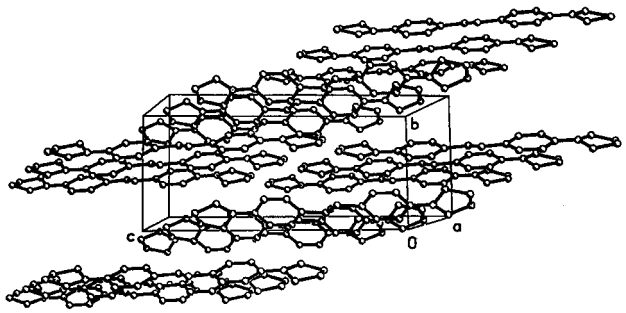

Fig. 5 Packing diagram of DPS.

molecules, stacking in pairs, form a layer-like structure along the *c* axis. Least-square plane calculations show that the central stilbene unit possesses perfect planarity, while the dihedral angle between stilbene and pyrrolidinyl ring is 8.6°, which is different from that of BDPAS due to the variation with terminal rings.

CCDC 154227. See http://www.rsc.org/suppdata/jm/b0/b009769l/ for crystallographic files in .cif format.

Calculations

Charge density distribution of the ground and the first excited states was calculated using the PM3 semi-empirical method. Dipole moment change between ground and first excited states ($\Delta\mu_{ge}$), and transition dipole moment between first and second excited states ($M_{ee'}$) were calculated using the ZINDO program.

Optical properties measurement

Linear optical properties. Linear absorption spectra for all chromophores in DMF with $d_0 = 1.0 \times 10^{-5}$ M have been measured in quartz cuvettes of 1 cm path on a Hitachi U-3500

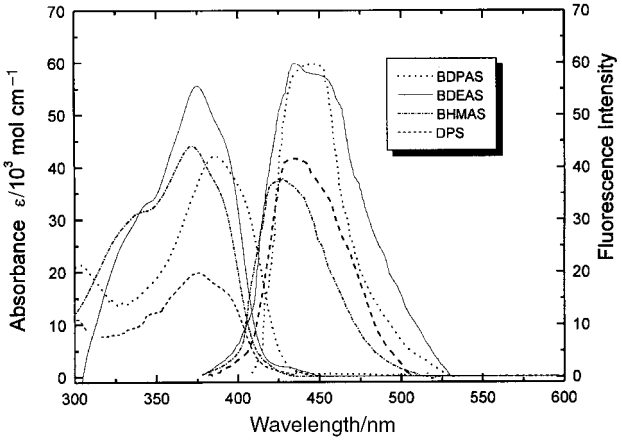

Fig. 6 Linear absorption and single-photon fluorescence spectra of BDPAS (dotted), BDEAS (solid), BHMAS (dash dotted), and DPS (dashed) in DMF solvent at $d_0 = 1 \times 10^{-5}$ M. Absorption spectra are the left ones and fluorescence spectra are the right ones in each pair (The fluorescence peak positions of BHMAS and DPS are red-shifted 20 nm compared with the original measured data).

recording spectrophotometer. One-photon induced fluorescence spectra of a Shimadzu RF5000U fluorophotometer at a concentration of 1.0×10^{-5} M in DMF or in other different solvents were recorded. These spectra are shown in Figs. 6–8.

Nonlinear optical properties. Two-photon absorptivitives of all the chromophores were measured by direct nonlinear optical transmission (NLT). An optical parameter amplifier (OPA) pumped by a mode-locked Nd:YAG laser was used as pumping source which can be tuned in the range of 400–2000 nm, while the input–output energy was measured by a two-channel energy-meter. The influences of the quartz cell and the linear absorption of the solvents have been subtracted. Then two-photon absorption coefficient, β (in units of cm GW^{-1}), was calculated by using measured nonlinear transmissivity (T_i) for a given input intensity (I_0) and thickness of a sample solution (L) from eqn. (1); finally, the two-photon absorption cross section, δ_{TPA} (in units of cm^4 s photon^{-1}) can be determined by eqn. (2),[22,23]

$$T_i = [\ln(1 + \beta L I_0)]/\beta L I_0 \quad (1)$$

$$\delta_{TPA} = h\nu\beta \times 10^3 / N_A C_0 \quad (2)$$

where N_A and C_0 are Avogadro's constant and the molar concentration of solute, respectively, and $h\nu$ is the energy of the incident photon. The calculated β and δ_{TPA} values are shown in Table 1.

Results and discussion

Linear absorption and single-photon fluorescence spectra

Figs. 6–8 present linear absorption and one-photon fluorescence spectra of symmetric and asymmetric chromophores, respectively. First of all, the absorption spectra of D-π-A compounds are noticeably red-shifted with respect to those of their symmetric counterparts. The peak absorption for symmetric stilbene derivatives is located at 374–387 nm (on the left side of Fig. 6), while those of asymmetric pyridinium derivatives are at ~480 nm, and quinolinium derivatives at ~550 nm (on the left side of Fig. 7). This due to the electronic interactions between donor and acceptor inducing a spectral shift to lower energy with respect to those between donor and donor. Along with the red shift of the absorptivities, one-photon fluorescence intensity of chromophores decreases drastically from symmetric molecules to pyridinium, and further to quinolinium derivatives. From the right of

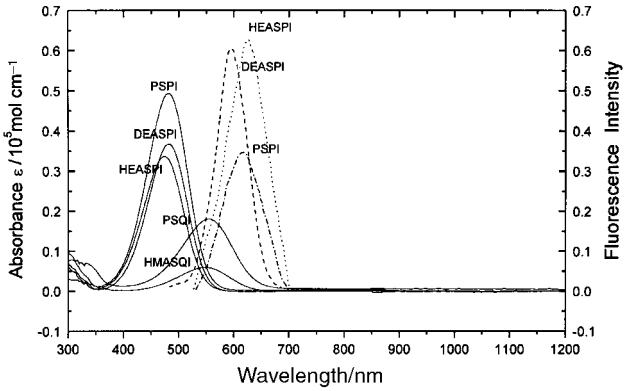

Fig. 7 Linear absorption of PSPI (solid), DEASPI (solid), HEASPI (solid), HMASQI (solid), and PSQI (solid) in DMF solvent at $d_0 = 1 \times 10^{-5}$ M, and single-photon fluorescence spectra of HEASPI (dotted), DEASPI (dashed) and PSPI (dash dotted) in DMF solvent at $d_0 = 1 \times 10^{-5}$ M.

Figs. 6–7, one can see that the relative fluorescence intensities for symmetric chromophores are almost 100 times as strong as those of their pyridinium counterparts, and for quinolinium derivatives, there is no detectable one-photon fluorescence. Since the measurement is performed under exactly the same conditions, the change of the relative fluorescence intensity means that the fluorescence quantum yields follow the same sequence: symmetric chromophores > pyridinium derivatives > quinolinium derivatives. This is probably due to a partial quenching[24] associated with a twisted intramolecular charge transfer (TICT) state. Since the structure of asymmetric molecules satisfies all the criteria of the TICT process, namely, an electron donor (disubstituted amino) and an aromatic acceptor moiety joined by a flexible bond, there is more tendency for asymmetric molecules to take part in a twisted charge transfer process than their symmetric counterparts. To examine further the different excited state emission behavior of the symmetric and asymmetric chromophores, the emission spectra of BDPAS and PSPI in various solvents were determined, and presented in Fig. 8. The molecular polarity parameters E_T (30)[25] are shown in Fig. 8 for the relevant solvents. It is interesting to note that there are quite different solvent effects between the symmetric and asymmetric chromophores. One can see from Fig. 8 that the asymmetric chromophore PSPI gives a red shift with an increase in solvent polarity parameter E_T (30), *e.g.* the maximum shifts from 567 nm in chloroform (E_T (30), 39.1), 590 nm in DMF (E_T (30), 43.8) to 599 nm in acetonitrile (E_T (30), 46.0), which is the same as noted for ASPI previously.[26] In contrast, the fluorescence spectra of symmetric BDPAS in different solvents exhibit a small red shift generally with decreasing solvent polarity parameter E_T (30), *e.g.*, the maximum shifts from 445 nm in benzyl alcohol (E_T (30), 50.8), 450 nm in DMF (E_T (30), 43.8), 420 nm in chloroform (E_T (30), 39.1), and to 470 nm in toluene (E_T (30), 33.9). It is interesting to note that asymmetric molecules in chloroform give the strongest emission while symmetric molecules in chloroform give the weakest, and in one case even quenches fluorescence completely. These results indicate that the asymmetric molecules are more polar in the excited state than in the ground state,[27] and an increase in the polarity of the solvent will lower the energy level of the charge transfer excited state. In addition, the TICT process, presumably favored in more polar solvents, will result in a pronounced decrease in the fluorescence yield.[27] The predicted dipole moments obtained by PM3 calculations confirm that the dipole moment of PSPI in the excited state is greater than that in the ground state by 3.4 D. In contrast, the difference in dipole moment ($\Delta\mu_{ge}$) for BDPAS is almost negligible. Therefore, the influence of the solvent effect upon the fluorescence behavior is different from that of the asymmetric counterparts.

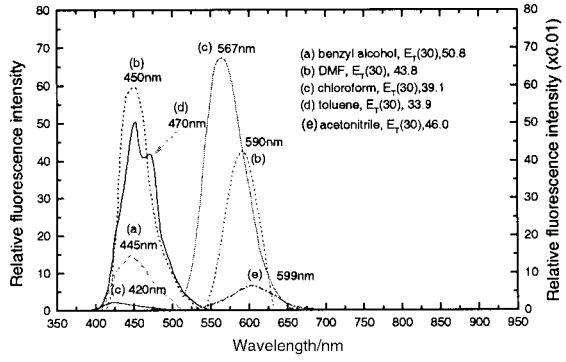

Fig. 8 One-photon induced fluorescence spectra for symmetric BDPAS (on the left) and symmetric PSPI (on the right) in various solvents with the same concentration of $d_0 = 1.0 \times 10^{-5}$ M. Curve (d) for PSPI is obtained by reducing the original measured data 10 times in the intensity scale.

Symmetric, asymmetric charge transfer process and two-photon absorption

Table 1 presents the calculated dipole moment difference between the ground and first excited state ($\Delta\mu_{ge}$) and transition dipole moment between the first and second excited states ($M_{ee'}$) for all chromophores. It is interesting that the symmetric chromophores all have a negligible $\Delta\mu_{ge}$ value, while the asymmetric counterparts show a large dipole moment difference. Moreover the variation in the transition dipole moment ($M_{ee'}$) for these two types of molecules also shows a different behavior, which we consider to originate from their intramolecular charge transfer character.

Calculated charge density distributions for the symmetric molecule DPS, as presented in Fig. 9 show that the charge transfer shifts from the central stilbene unit to the two terminal substituted amino group in the S_0 ground state, that is, $Q_{amino} = -0.0255e$ and $Q_{centr} = +0.0510e$, whereas in the S_1 state the charge transfer process is reversed, shifting from the two terminal groups to the central stilbene moiety, that is, $Q_{amino} \cong +0.031e$ and $Q_{centr} \cong -0.062e$. Although such a symmetric charge transfer behavior results in a negligible $\Delta\mu_{ge}$ value, it can greatly affect the quadrupole moment, which is beneficial in enhancing the corresponding transition dipole moment $(M_{ee'})^2$ (seen in Table 1). In contrast, for the asymmetric quinolinium or pyridinium derivatives there is a

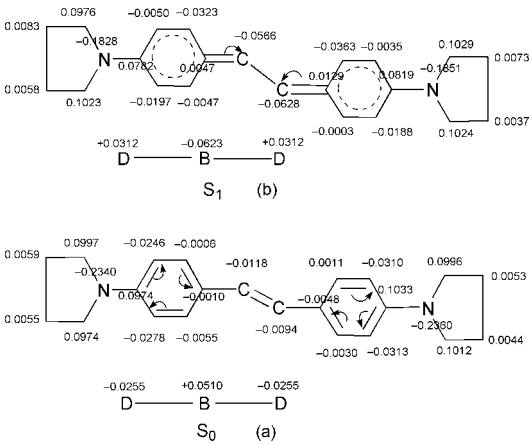

Fig. 9 PM3-optimized charge density (e) for DPS in the S_0 (a) and S_1 (b) states. The individual charge densities on the molecular backbone represent the summations of the charge densities on each carbon atom and the hydrogen atom(s) attached. D and B provide the total charge on the amino group and the stilbene bridge, respectively.

Table 1 Nonlinear optical properties and calculated structural parameters for symmetric and asymmetric chromophores

Chromophores		$\Delta\mu_{ge}$/debye	$M_{ee'}$/debye	β_{TPA}/cm GW^{-1}	δ_{TPA} ($\times 10^{-48}$) cm^4 s photon^{-1}	$\lambda^{max}{}_{TPA}$/nm (solvent, d_0)
D-π-D	DPS	0.02	13.6	1.19	57.7	600 (toluene, 0.0005 M)
	BHMAS	0.03	13.0	0.81	44.5	590 (DMF, 0.005 M)
	BDEAS	0.04	14.4	1.37	62.0	730 (toluene, 0.005 M)
	BDPAS	0.01	12.2	0.68	39.4	730 (toluene, 0.005 M)
D-π-A	PSPI	3.4	8.5	4.04	28.5	930 (DMF, 0.05 M)
	HEASPI	8.2	8.6	3.38	24.0	930 (DMF, 0.05 M)
	DEASPI	8.1	8.2	4.47	38.8	930 (DMF, 0.05 M)
	PSQI	10.0	7.3	0.07	26.8	970 (DMF, 0.001 M)
	HMASQI	10.6	8.7	0.15	48.5	1010 (DMF, 0.001 M)

major asymmetry of charge density distribution. For example, the charge distribution of PSPI, presented in Fig. 10, shows that there exists a strong dipolar character, directing from the substituted amino group to the acceptor group in the S_0 state, that is, $Q_D = +0.2133e$ and $Q_A = -0.2611e$. Further charge separation occurs in the excited state, that is, $Q_D = +0.6670e$ and $Q_A = -0.8365e$. Similar results were also obtained for all the other asymmetric molecules. Clearly, such a charge transfer behavior results in a large difference in dipole moment ($\Delta\mu_{ge}$) between the ground and first excited state (see in Table 1).

It is accepted that the molecular TPA cross section, δ_{TPA}, is proportional to the imaginary part of the third-order polarizability,[2] and if the frequency (ω) is neglected, the third-order

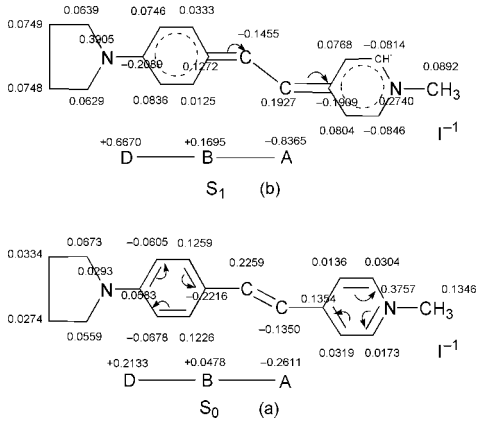

Fig. 10 PM3-optimized charge density (e) for PSPI in the S_0 (a) and S_1 (b) states. The individual charge densities on the molecular backbone represent the summations of the charge densities on each carbon atom and the hydrogen atom(s) attached. D, B, and A provide the total charge on the amino group, the styryl bridge and the acceptor, respectively.

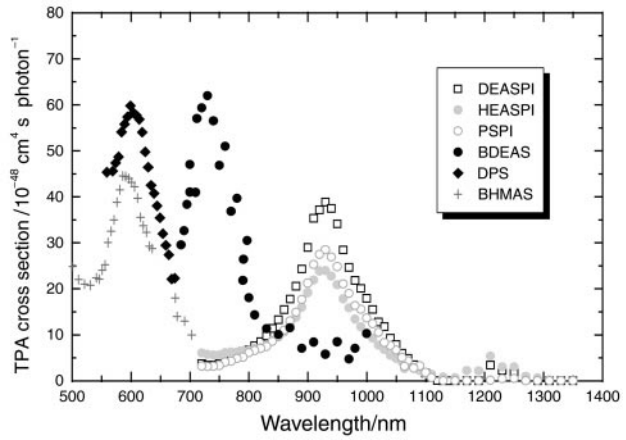

Fig. 11 The TPA cross sections (δ_{TPA}) for parts of chromophores in DMF ($d_0 = 0.05$ M) for PSPI, DEASPI and HEASPI; and in DMF ($d_0 = 0.005$ M) for BHMAS, in toluene ($d_0 = 0.005$ M) for BDEAS and BDPAS, in toluene ($d_0 = 0.0005$ M) for DPS.

polarizability, γ, can be expressed as eqn. (3),[28,29]

$$\delta_{TPA} \propto \gamma_{xxxx} = 24 \frac{M_{ge}^2}{E_{ge}^2}\left[\frac{\Delta\mu_{ge}^2}{E_{ge}} + \sum_{e'} \frac{M_{ee'}^2}{E_{ge'}^2} - \frac{M_{ge}^2}{E_{ge}}\right] \quad (3)$$

Therefore, the δ_{TPA} value depends on the ground state to first excited state dipole moment change ($\Delta\mu_{ge}$), the transition dipole moment between the first and second excited state ($M_{ee'}$) and the energy differences between the ground and the excited states (E_{ge}, or $E_{ge'}$), *etc.*

It is understandable that the difference of symmetric or asymmetric charge transfer for structural parameters may result in the variation in molecular two-photon absorptivity. As shown in Table 1, the symmetric structural chromophores exhibit TPA cross sections almost twice as large as those of their asymmetric counterparts. For example, the δ_{TPA} values vary from 62.0×10^{-48} cm^4 s photon^{-1} for BDEAS, to 38.8×10^{-48} cm^4 s photon^{-1} for DEASPI. When the donor group is pyrrolidinyl, the δ_{TPA} values vary from 57.7×10^{-48} cm^4 s photon^{-1} for DPS, to 28.5×10^{-48} cm^4 s photon^{-1} for PSPI, and 26.8×10^{-48} cm^4 s photon^{-1} for PSQI. When the donor group is *N*-hydroxyethyl-*N*-alkylamino, the δ_{TPA} values vary from 44.5×10^{-48} cm^4 s photon^{-1} for BHMAS, to 24.0×10^{-48} cm^4 s photon^{-1} for HEASPI. Though the symmetric chromophores have a negligible dipole moment change ($\Delta\mu_{ge}$), they exhibit larger δ_{TPA} values and we can assume that the transition dipole moment ($M_{ee'}$) function plays a much more important role in enhancement of the δ_{TPA} value. With an increase of $M_{ee'}$ value, the symmetric molecules possess the same sequence in their δ_{TPA} values: BDEAS > DPS > BHMAS > BDPAS, which means that the δ_{TPA} value is proportional to the amount of intramolecular charge transfer. In the case of their asymmetric counterparts, any simultaneous increase of $M_{ee'}$ and $\Delta\mu_{ge}$ serves to increase their δ_{TPA} values. It is for this reason that HMASQI and DEASPI exhibit relatively large δ_{TPA} values. As for PSPI and PSQI, the large δ_{TPA} value for PSPI is due to its larger $M_{ee'}$ value. As for HEASPI, its relatively large E_{ge} (seen in Fig. 7) can contribute to making its δ_{TPA} value smaller.

It is interesting to compare the effect of the type of symmetry on the TPA peak positions, shown in Fig. 11 and Table 1. The peak positions for symmetric molecules are located at 590–730 nm, while those for the asymmetric counterparts are located at 930–1010 nm, that is, at nearly twice the wavelength value of their corresponding one-photon absorption peak. Comparing DPS, BHMAS and BDEAS, as shown in Fig. 6 and Fig. 11, one can see that although their linear absorption peaks ($\lambda^{(1)}{}_{max}$) are all at ~374 nm, the two-photon absorption peaks ($\lambda^{(2)}{}_{max}$) are observed at 730 nm for BDEAS, and 600 nm for DPS, and 590 nm for BHMAS. Thus BDEAS exhibits a significant red shift of its two-photon absorptivity. A similar red shift also occurs in the asymmetric quinolinium derivatives. For example, the $\lambda^{(1)}{}_{max}$ of HMASQI and PSQI lie at ~550 nm, but the $\lambda^{(2)}{}_{max}$ is at 1010 nm for HMASQI and 970 nm for PSQI (seen in Fig. 7 and Table 1). Such a bathochromic shift of the two-photon absorptivity for

BDEAS and HMASQI suggests that they possess the stabilization of the second excited state (*i.e.* small $E_{ge'}$), which contributes to the two-photon absorptivity (see eqn. (3)).

Conclusions

A comparative study of electronically symmetrical and electronically asymmetrical charge-transfer chromophores of the D-π-D and D-π-A types respectively is reported. It was interesting to note that the molecular structural symmetry exerts a markedly different behavior on the linear and nonlinear optical properties of the chromophores.

Solvent effect studies have shown that the asymmetric chromophores are more polar in the excited state than in the ground state while symmetric counterparts behave differently. There is a trend for the asymmetric chromophores to take part in a twisted charge transfer process more readily than their symmetric counterparts, so the one-photon fluorescence intensity for the asymmetric molecules is dramatically decreased, in comparison with their symmetric counterparts.

The influence of the direction of the intramolecular charge transfer process, *i.e.*, symmetric and asymmetric, on the two-photon absorption cross section has been theoretically and experimentally demonstrated. We have shown that asymmetric chromophores exhibit relatively larger ground state–first excited state dipole moment change ($\Delta\mu_{ge}$), whilst their symmetric counterparts exhibit relatively larger transition dipole moments between the first and second excited states ($M_{ee'}$). Although a high TPA cross section is provided by the simultaneously high values of $M_{ee'}$ and $\Delta\mu_{ge}$, the former parameter is more important. As a consequence, the symmetric molecules exhibit larger δ_{TPA} values compared to their asymmetric counterparts.

Acknowledgements

This work was supported by a grant from the State Key Program of China.

References

1 J. D. Bhawalkar, G. S. He and P. N. Prasad, *Prog. Phys*, 1996, **59**, 1041.
2 M. Albota, D. Beljonne, J.-L. Bredas, J. E. Ehrlich, J.-Y. Fu, A. A. Heikal, S. E. Hess, T. Kogej, M. D. Levin, S. R. Marder, D. McCord-Maughon, J. W. Perry, H. R. Rumi, G. Subramaniam, W. W. Webb, X.-L. Wu and C. Xu, *Science*, 1998, **281**, 1653.
3 D. Beljonne, J. L. Brédas, M. Cha, W. E. Torruellas, G. I. Stegeman, J. W. Hofstraat, W. H. G. Horsthuis and G. R. Möhlmann, *J. Chem. Phys.*, 1995, **103**, 7835.
4 J. E. Ehrlich, X. L. Wu, I.-Y. S. Lee, Z.-Y. Hu, H. Röckel, S. R. Marder and J. W. Perry, *Opt. Lett.*, 1997, **22**, 1843.
5 G. S. He, R. Gvishi, P. N. Prasadl and B. A. Reinhardt, *Opt. Commun.*, 1995, **117**, 133.
6 C. W. Spangler, *J. Mater. Chem.*, 1999, **9**, 2013.
7 B. H. Cumpston, S. P. Ananthavel, S. Barlow, D. L. Dyer, j. E. Ehrlich, L. L. Erskine, A. A. Heikal, S. R. Kuebler and J. W. Perry, *Nature*, 1999, **51**, 398.
8 D. A. Parthenopoulos and P. M. Rentzepis, *Science*, 1989, **245**, 843.
9 W. Denk, J. H. Strickler and W. W. Webb, *Science*, 1990, **73**, 248.
10 S. Maruo, O. Nakamura and S. Kawata, *Opt. Lett.*, 1997, **22**, 132.
11 E. S. Wu, J. H. Strickler, W. R. Harrell and W. W. Webb, *Proc. C. F. SPIE-Int. Soc. Opt. Eng.*, 1992, **1674**, 776.
12 C. F. Zhao, G. S. He, J. D. Bhawalkar, C. K. Park and P. N. Prasad, *Chem. Mater.*, 1995, **7**, 1979.
13 G. S. He, L. X. Yuan, Y. P. Cui, M. Li and P. N. Prasad, *J. Appl. Phys.*, 1997, **81**, 2529.
14 G. S. He, K. S. Kim, L. X. Yuan, N. Cheng and P. N. Prasad, *Appl. Phys. Lett.*, 1997, **71**, 1619.
15 H. Stiel, K. Tenchner, A. Paul, W. Freyer and D. Leupold, *J. Photochem. Photobiol A: Chem.*, 1994, **80**, 289.
16 J. D. Bhawalkar, G. S. He and C. K. Park, *Opt. Commun.*, 1996, **124**, 33.
17 G. S. He, R. Signorini and P. N. Prasad, *App. Opt.*, 1998, **37**, 5720.
18 S. H. G, L. Yuan and P. N. Prasad, *Opt. Commun.*, 1997, **140**, 49.
19 B. A. Reinhardt, L. L. Brott, S. J. Clarson, A. G. Dillard and J. C. Bhatt, *Chem. Mater.*, 1998, **10**, 1863.
20 X. M. Wang, C. Wang, W. T. Yu, Y. F. Zhou, X. Zhao, Q. Fang and M. H. Jiang, *Can. J. Chem.*, 2001, **79**, in press.
21 X. M. Wang, Y. F. Zhou, W. T. Yu, C. Wang, Q. Fang, M. H. Jiang, H. Lei and H. Z. Wang, *J. Mater. Chem.*, 2000, **10**, 2698.
22 G. S. He, L. Yuan, N. Cheng, J. D. Bhawalkar, P. N. Prasad, L. L. Brott, S. J. Clarson and B. A. Reinhardt, *J. Opt. Soc. Am., B.*, 1997, **14**, 1079.
23 L. W. Tutt and T. F. Boggess, *Quantum Electron.*, 1993, **17**, 2279.
24 O.-K. Kim and J.-M. Lehn, *Chem. Phys. Lett.*, 1996, **255**, 147.
25 C. Reichardt, *Angew. Chem., Int. Ed. Engl.*, 1979, **18**, 98.
26 G. S. He, L. Yuan, Y. P. Cui, M. Li and P. N. Prasad, *J. Appl. Phys.*, 1997, **81**, 2529.
27 N. Sarkar, K. Das, D. N. Nath and K. Bhattacharyya, *Langmuir*, 1994, **10**, 326.
28 F. Meyers, S. R. Marder, B. M. Pierce and J. L. Brédas, *J. Am. Chem. Soc.*, 1994, **116**, 10703.
29 T. Kogej, D. Beljonne, F. Meyyers, J. W. Perry, S. R. Marder and J. L. Brédas, *Chem, Phys Lett.*, 1998, **298**, 1.